Electrically Conducting Materials Based On μ-Tetrathiooxalato-Bridged Bimetallic Ni(II) Anionic Complexes

Anthony E. Pullen,[†] Stephan Zeltner,[‡] Ruth-Maria Olk,[‡] Eberhard Hoyer,[‡] Khalil A. Abboud,[†] and John R. Reynolds*[,†]

Department of Chemistry, Center for Macromolecular Science and Engineering, University of Florida, Gainesville, Florida 32611-7200, and Institut für Anorganische Chemie, Universität Leipzig, Talstrasse 35, D-04103 Leipzig, FRG

Received January 31, 1997[⊗]

A series of μ-tto- (tto = $C_2S_4^{2-}$ = tetrathiooxalato) bridged bimetallic Ni(II) complexes with the general formula $(Y)_2\{tto[Ni(L)]_2\}$ (where Y = Bu_4N^+, L = dsit = $C_3Se_2S_3^{2-}$ = 2-thioxo-1,3-dithiole-4,5-diselenolato (**2**) and dmise = $C_3SeS_4^{2-}$ = 2-selenoxo-1,3-dithiole-4,5-dithiolato (**3**); and where Y = Me_4N^+ (**4**) and Et_4N^+ (**5**), L = dmit = $C_3S_5^{2-}$ = 2-thioxo-1,3-dithiole-4,5-dithiolato) have been synthesized. The single-crystal X-ray structures of **2**, **3**, **4** and **5** have been determined: **2**, $(Bu_4N)_2\{tto[Ni(dsit)]_2\}$, monoclinic, space group $P2_1/c$, a = 9.8893(1) Å, b = 15.3544(1) Å, c = 17.8825(2) Å, β = 90.561(1)°, Z = 2; **3**, $(Bu_4N)_2\{tto[Ni(dmise)]_2\}$, orthorhombic, space group $P2_12_12_1$, a = 9.8286(2) Å, b = 16.1741(3) Å, c = 34.3022(1) Å, Z = 4; **4**, $(Me_4N)_2\{tto[Ni(dmit)]_2\}$, monoclinic, space group $C2/m$, a = 13.8043(4) Å, b = 10.1081(1) Å, c = 12.0483(3) Å, β = 115.239(1)°, Z = 2; **5**, $(Et_4N)_2\{tto[Ni(dmit)]_2\}$, monoclinic, space group $P2_1/n$, a = 11.8313(1) Å, b = 11.0172(2) Å, c = 15.3014-(1) Å, β = 110.951(1)°, Z = 2. All of the complexes presented are extensively conjugated and chalcogen-rich with $(Bu_4N)_2\{tto[Ni(dsit)]_2\}$ (**2**), $(Bu_4N)_2\{tto[Ni(dmise)]_2\}$ (**3**), and $(Me_4N)_2\{tto[Ni(dmit)]_2\}$ (**4**) also being planar as precursors to electrically conducting materials. The angle of the tto−Ni−L portion of the complexes varies with the choice of ligand and with the counterion. Cyclic voltammetry results of **2** and **3** each show a first low-potential reversible redox couple followed by a second nonreversible redox couple. The structural and electronic properties of **2**−**5** are compared to those of the recently communicated analogous complex, $(Bu_4N)_2$-$\{tto[Ni(dmit)]_2\}$ (**1**). Electrocrystallization, interdiffusion, and chemical oxidation experiments with **1** have yielded black insoluble materials with high pressed powder conductivities of up to 0.5 S/cm.

Introduction

Transition metal complexes containing chalcogen-rich ligands have received significant attention in the synthesis of molecular electrical conductors or so-called "synthetic metals". Since the discovery of the first organic metal TTF−TCNQ (TTF = tetrathiafulvalene, TCNQ = 7,7,8,8-tetracyano-*p*-quinodimethane) in 1973,[1] several systems have been synthesized to "mock" the TTF structure to potentially find other systems that will result in metallic or even superconducting properties. The transition metal based system that has been most thoroughly studied is $[M(dmit)_2]^{n-}$ (where M = Ni, Pd, or Pt; dmit = $C_3S_5^{2-}$ = 2-thioxo-1,3-dithiole-4,5-dithiolato; $0 \le n \le 2$).[2] Using square planar coordinating metals, the complex is planar, π delocalized and the large sulfur orbitals result in close-packed systems with a large degree of intermolecular overlap. This promotes the formation of a delocalized band structure, a prerequisite for the making of a material with metallic or superconducting electrical properties.[3] The $M(dmit)_2$ (when M = Ni or Pd) unit with both closed-shell and open-shell counterions has formed seven superconducting salts to date.[4] All of them superconduct at rather low temperatures (<5 K), only one of which does not require high pressure to do so.[4j]

Keeping with the structural characteristics that contributed to the formation of $M(dmit)_2$-based superconductors, we report a new series of chalcogen-rich, extensively conjugated and planar bimetallic Ni(II) complexes with the general formula $(Y)_2$-$\{tto[Ni(L)]_2\}$ (tto = $C_2S_4^{2-}$ = tetrathiooxalato; when Y = Bu_4N^+ = tetrabutylammonium, L = dmit (**1**), dsit = $C_3Se_2S_3^{2-}$ = 2-thioxo-1,3-dithiole-4,5-diselenolato (**2**), dmise = $C_3SeS_4^{2-}$ = 2-selenoxo-1,3-dithiole-4,5-dithiolato (**3**); when Y = Me_4N^+ = tetramethylammonium, L = dmit (**4**); and when Y = Et_4N^+ = tetraethylammonium, L = dmit (**5**)). The complexes have been designed to extend the intramolecular delocalization and

* To whom correspondence should be addressed.
† University of Florida.
‡ Universität Leipzig.
⊗ Abstract published in *Advance ACS Abstracts,* August 1, 1997.

(1) Ferraris, J. P.; Cowan, D. O.; Valatka, V.; Perlstein, J. H. *J. Am. Chem. Soc.* **1973**, *95*, 948.
(2) (a) Shklover, V. E.; Nagapetyan, S. S.; Struchkov, Y. T. *Usp. Khim.* **1990**, *59*, 1179. (b) Cassoux, P.; Interrante, L. V. *Comments Inorg. Chem.* **1991**, *12*, 47. (c) Cassoux, P.; Valade, L.; Kobayashi, H.; Kobayashi, A.; Clark, R. A.; Underhill, A. E. *Coord. Chem. Rev.* **1991**, *110*, 15. (d) Olk, R. M.; Olk, B.; Dietzsch, W.; Kirmse, R.; Hoyer, E. *Coord. Chem. Rev.* **1992**, *17*, 99. (e) Cassoux, P.; Valade, L. In *Inorganic Materials*; J. Wiley and Sons: Chichester, England, 1992. (f) Williams, J. M.; Ferraro, J. R.; Thorn, R. J.; Carlson, K. D.; Geiser, U.; Wang, H. H.; Kini, A. M.; Whangbo, M. H. *Organic Superconductors (Including Fullerenes)*; Prentice Hall: Englewood Cliffs, NJ, 1992.
(3) Alvarez, S.; Vicente, R.; Hoffmann, R. *J. Am. Chem. Soc.* **1985**, *107*, 6253.
(4) (a) Bousseau, M.; Valade, L.; Legros, J. P.; Cassoux, P.; Garbauskas, M.; Interrante, L. V. *J. Am. Chem. Soc.* **1986,** *108*, 1908. (b) Brossard, L.; Ribault, M.; Bousseau, M.; Valade, L.; Cassoux, P. *C. R. Acad. Sci. (Paris), Sér. II* **1986**, *302*, 205. (c) Brossard, L.; Ribault, M.; Valade L.; Cassoux, P. *Physica B & C (Amsterdam)* **1986**, *143*, 378. (d) Kobayashi, A.; Kim, A.; Sasaki, Y.; Kato, R.; Kobayashi, H.; Moriyama, S.; Nishio, Y.; Kajita, K.; Sasaki, W. *Chem. Lett.* **1987**, 1819. (e) Kajita, K.; Nishio, Y.; Moriyama, S.; Kato, R.; Kobayashi, H.; Sasaki, W. *Solid State Commun.* **1988**, *65*, 361. (f) Brossard, L.; Hurdequint, H.; Ribault, M.; Valade, L.; Legros, J. P.; Cassoux, P. *Synth. Met.* **1988**, *27*, B157. (g) Brossard, L.; Ribault, M.; Valade, L.; Cassoux, P. *J. Phys. (Paris)* **1989**, *50*, 1521. (h) Kobayashi, A.; Kobayashi, H.; Miyamoto, A.; Kato, R.; Clark, R. A.; Underhill, A. E. *Chem. Lett.* **1991**, 2163. (i) Kobayashi, H.; Bun, K.; Naito, T.; Kato, R.; Kobayashi, A.*Chem. Lett.* **1992**, 1909. (j) Tajima, H.; Inokuchi, M.; Kobayashi, A.; Ohta, T.; Kato, R.; Kobayashi, H.; Kuroda, H. *Chem. Lett*. **1993**, 1235.

S0020-1669(97)00121-3 CCC: $14.00

increase intermolecular interactions in the crystal lattice. Complexes **1**, **3**, and **4** are the first fully planar bimetallic μ-tetrathiooxalato-bridged Ni(II) compounds synthesized.

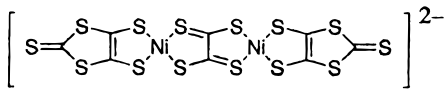

$\{tto[Ni(dmit)]_2\}^{2-}$ (**1**, **4**, **5**)

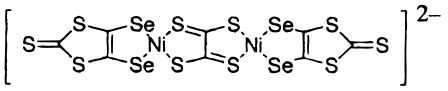

$\{tto[Ni(dsit)]_2\}^{2-}$ (**2**)

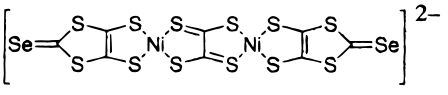

$\{tto[Ni(dmise)]_2\}^{2-}$ (**3**)

In 1982, Dahl and co-workers reported the first crystallographically shown example of coordinated tetrathiooxalate in the compound $Ni_2(\eta^5\text{-}C_5Me_5)_2(C_2S_4)$.[5] In this complex, the tetrathiooxalate ligand bridges Ni(II) metal centers containing the bulky $\eta^5\text{-}C_5Me_5$ ligand. The complex was formed from a metal-promoted reductive dimerization, followed by coordination of carbon disulfide. Another recently reported example of $\mu\text{-}C_2S_4$ bridging of Ni(II) metal centers was in 1994 by Rauchfuss and co-workers. They reported the complex $(Et_4N)_2[Ni_2C_2S_4\{S_2C_2S_2C_2(CO_2Me)_2\}_2]$, which was formed from the oxidation of the bis-chelate $[Ni_2C_2S_4\{S_2C_2S_2C_2(CO_2Me)_2\}_2]^{2-}$ when exposed to air in acetonitrile.[6a] This complex contains terminal out-of-plane ester groups preventing close intermolecular contacts. In related work, McCullough et al.[6b,c] have reported conjugated bimetallic compounds using the tetrathiafulvalenetetrathiolate bridging ligand. During the revision of this manuscript, we have learned that Bryce et al.[6d] have synthesized the oxygen-terminated $\{tto[Ni(dmid)]_2\}^{2-}$.

Recently, we reported a series of similar μ-tto-bridged bimetallic Cu(II) complexes with the general formula $(Bu_4N)_2\{tto[Cu(L)]_2\}$ (L = dmit (**6**), mnt = $C_4N_2S_2^{2-}$ = 1,2-dicyanoethene-1,2-dithiolato (**7**), dsit (**8**), and dmid = $C_3OS_4^{2-}$ = 2-oxo-1,3-dithiole-4,5-dithiolato (**9**)).[7] Complex **7** with mnt as the capping ligand is the first reported completely planar complex with tetrathiooxalate-bridged Cu(II) metal centers.

Herein are presented the synthesis, X-ray structure analyses, and electrochemical behavior of **2**−**5**. These results will be compared to those for the previously communicated complex $(Bu_4N)_2\{tto[Ni(dmit)]_2\}$[8] (**1**) along with the bimetallic Cu(II) complexes **6**−**9**. Also, electrically conducting complexes using **1** have been prepared via slow interdiffusion, chemical oxidation, and electrocrystallization experiments.

Experimental Section

General Procedures. Melting points were determined using a Fisher-Johns hot stage melting point apparatus and are uncorrected. Infrared spectra were recorded on a Perkin-Elmer 1310 IR spectrophotometer and a Perkin-Elmer 1600 FTIR spectrophotometer. UV−vis spectra were recorded on a Shimadzu UV-160A spectrophotometer. Elemental analyses were completed at the University of Leipzig, FRG, on a Hereaus CHN rapid analyzer and at Robertson Microlit Labs, Madison, NJ. The X-ray crystal structure analyses were carried out at the University of Florida.

Materials. All solvents were thoroughly degassed with argon prior to use, and the acetonitrile was additionally dried and distilled over calcium hydride. All reactions were completed under an argon atmosphere. Tetraethylammonium tetrathiooxalate, $(Et_4N)_2tto$,[9] Cs_2dsit,[10] Cs_2dmise,[10b,11] and $(Bu_4N)_2\{tto[Ni(dmit)]_2\}$ (**1**)[8,10b] were prepared as described in the literature.

Preparation of $(Bu_4N)_2\{tto[Ni(dsit)]_2\}$ (2). To 75 mL of acetone were added Cs_2dsit (0.278 g, 0.500 mmol), Bu_4NBr (0.193 g, 0.600 mmol), and $(Et_4N)_2tto$ (0.103 g, 0.250 mmol), and the mixture was stirred for 10 min. A solution of $NiCl_2\cdot 6H_2O$ (0.119 g, 0.500 mmol) in a minimal amount of methanol was slowly added to the stirring solution with a pipet. The solution was then stirred for approximately 45 min and filtered to remove undissolved $(Et_4N)_2tto$ or insoluble oligomeric $[Ni(tto)]_n$. To the filtrate was added approximately 25 mL of 2-propanol, and the solution was allowed to evaporate to less than one-fourth of the initial volume overnight. The crystalline product was then filtered using gravity filtration, and CH_2Cl_2 was added in small amounts until any green colored solution ($[Ni(dsit)_2]^{2-}$) no longer separated. The remaining product was recrystallized in 1:1 acetone/2-propanol to yield $(Bu_4N)_2\{tto[Ni(dsit)]_2\}$ (**2**) as dark brown-black platelet-like crystals. Yield: 117 mg (41%). Mp: 247−249 °C dec. Anal. Calcd for $C_{40}H_{72}N_2Ni_2Se_4S_{10}$: C, 35.99; H, 5.44; N, 2.10; S, 24.02. Found: C, 36.19; H, 5.66; N, 2.44; S, 24.12. IR (KBr; cm^{-1}): ν(C−H) 2948, 2867; ν(C═C) 1476, 1376; ν(C═S) 1056, 986. UV−vis [acetone; λ, nm (log ϵ)]: 390 (4.80), 446 (4.26), 501 (4.09), 1053 (4.20).

$(Bu_4N)_2\{tto[Ni(dmise)]_2\}$ (3). The synthetic procedures are similar to those used for the synthesis of **2** but with Cs_2dmise (0.254 g, 0.500 mmol) instead of Cs_2dsit. The product remaining after evaporation and gravity filtration was again purified by addition of small amounts of methylene chloride to remove dark-green colored $[Ni(dmise)_2]^{2-}$ byproduct that may have formed during the synthesis of **3**. The remaining solid was then recrystallized in 1:1 acetone/2-propanol to yield $(Bu_4N)_2\{tto[Ni(dmise)]_2\}$ (**3**) as dark brown-black platelet-like crystals. Yield: 100 mg (32%). Mp: 298−300 °C dec. Anal. Calcd for $C_{40}H_{72}N_2Ni_2Se_2S_{12}$: C, 38.71; H, 5.86; N, 2.26; S, 31.00. Found: C, 38.25; H, 5.59; N, 2.21; S, 30.67. IR (KBr: cm^{-1}): ν(C−H) 2956, 2869; ν(C═C) 1467, 1412; ν(C═S) 959. UV−vis [acetone; λ, nm (log ϵ)]: 384 (4.64), 489 (4.18), 552 (4.19), 1061 (4.24).

$(Me_4N)_2\{tto[Ni(dmit)]_2\}$ (4). To 20 mL of a 0.100 M solution of Me_4NClO_4 in acetonitrile was added $(Bu_4N)_2\{tto[Ni(dmit)]_2\}$ (**1**) (0.030 g, 0.026 mmol), and the mixture was stirred for approximately 15 min to dissolve **1**, followed by filtration. The filtrate was then allowed to sit under an argon atmosphere for 48 h. The lesser soluble $(Me_4N)_2\{tto[Ni(dmit)]_2\}$ (**4**) crystallized out as black chunk-like crystals. Yield: 2 mg (10%). Mp: >300 °C. Anal. Calcd for $C_{16}H_{24}N_2Ni_2S_{14}$: C, 23.70; H, 2.99; N, 3.46; S, 55.37. Found: C, 23.89; H, 2.98; N, 3.36; S, 54.68. IR (KBr; cm^{-1}): ν(C−H) 2950, 2866; ν(C═C) 1453, 1380; ν(C═S) 1077, 960.

$(Et_4N)_2\{tto[Ni(dmit)]_2\}$ (5). The synthetic procedures are similar to those used for the synthesis of **4**. The electrolyte used was Et_4NBr, and the solvent was acetonitrile. The lesser soluble $(Et_4N)_2\{tto[Ni(dmit)]_2\}$ (**5**) crystallized out as black chunk-like crystals. Yield: 2 mg (8%). Mp: >300 °C. Anal. Calcd for $C_{24}H_{40}N_2Ni_2S_{14}$: C, 31.23;

(5) Maj, J. J.; Rae, A. D.; Dahl, L. F. *J. Am. Chem. Soc.* **1982**, *104*, 4278.
(6) (a) Yang, X.; Doxsee, D. D.; Rauchfuss. T. B.; Wilson, S. R. *J. Chem. Soc., Chem. Commun.* **1994**, 821. (b) McCullough, R. D.; Belot, J. A. *Chem. Mater.* **1994**, *6*, 1396. (c) McCullough, R. D.; Belot, J. A.; Rheingold, A. L.; Yap, G. P. A. *J. Am. Chem. Soc.* **1995**, *117*, 9913. (d) Batsnnov, A. S.; Bryce, M. B.; Dhindsa, A. S.; Howard, J. A. K.; Underhill, A. E.; *J. Mater. Chem. Commun.*, submitted for publication.
(7) (a) Piotraschke, J.; Pullen, A. E.; Abboud, K. A.; Reynolds, J. R. *Inorg. Chem.* **1995**, *34*, 4011. (b) Pullen, A. E.; Zeltner, S.; Olk, R. M.; Hoyer, E.; Abboud, K. A.; Reynolds, J. R. *Inorg. Chem.* **1996**, *35*, 4420.
(8) Pullen, A. E.; Olk, R. M.; Zeltner, S.; Hoyer, E.; Abboud, K. A.; Reynolds, J. R. *Inorg. Chem.* **1997**, *36*, 958.
(9) Jeroschewski, P. *Z. Chem.* **1981**, *21*, 412.
(10) (a) Zeltner, S.; Olk, R. M.; Pink, M.; Jelonek, S.; Jorchel, P.; Gelbrich, T.; Sieler, J.; Kirmse, R. *Z. Anorg. Allg. Chem.*, in press. (b) Gasiorowski, R.; Jorgensen, T.; Moller, J.; Hansen, T. K.; Pietraszkiewicz, M.; Becher, J. *Adv. Mater.* **1992**, *4*, 568.
(11) Zeltner, S.; Dietzsch, W.; Olk, R. M.; Kirmse, R.; Richter, R.; Schröder, U.; Olk, B.; Hoyer, E. *Z. Anorg. allg. Chem.* **1994**, *620*, 1768.

Table 1. Crystallographic Data for $(Bu_4N)_2\{tto[Ni(dsit)]_2\}$ (**2**), $(Bu_4N)_2\{tto[Ni(dmise)]_2\}$ (**3**), $(Me_4N)_2\{tto[Ni(dmit)]_2\}$(**4**), and $(Et_4N)_2\{tto[Ni(dmit)]_2\}$ (**5**)

	2	**3**	**4**	**5**
empirical formula	$C_{40}H_{72}N_2Ni_2S_{10}Se_4$	$C_{40}H_{72}N_2Ni_2S_{12}Se_2$	$C_{16}H_{24}N_2Ni_2S_{14}$	$C_{24}H_{40}N_2Ni_2S_{14}$
fw	1334.86	1241.06	810.63	922.84
space group	$P2_1/c$	$P2_12_12_1$	$C2/m$	$P2_1/n$
a, Å	9.8893(1)	9.8286(2)	13.8043(4)	11.8313(1)
b, Å	15.3544(1)	16.1741(3)	10.1081(1)	11.0172(2)
c, Å	17.8825(2)	34.3022(1)	12.0483(3)	15.3014(1)
β, deg	90.561(1)	90	115.239(1)	110.951(1)
V, Å^3	2715.23(4)	5452.98(2)	1520.67(6)	1862.64(4)
T, K	173(2)	173(2)	173(2)	173(2)
Z	2	4	2	2
λ, Å (Mo Kα)	0.710 73	0.710 73	0.710 73	0.710 73
ρ_{calc}, g cm^{-3}	1.633	1.512	1.770	1.645
μ, mm^{-1}	3.789	2.515	2.213	1.818
$R_1(F_o)$,[a] %	3.19	4.14	3.38	2.60
$R_2(F_o^2)$,[b] %	7.03	9.48	8.13	6.22

[a] $R_1 = \Sigma(||F_o| - |F_c||)/\Sigma|F_o|$. [b] $R_2 = [\Sigma[w(F_o^2 - F_c^2)^2]/\Sigma[w(F_o^2)^2]]^{1/2}$; $w = 1/[\sigma^2(F_o^2) + (0.0370p)^2 + 0.31p]$, $p = [\max(F_o^2,0) + 2F_c^2]/3$.

H, 4.38; N, 3.04; S, 48.64. Found: C, 31.00; H, 4.31; N, 2.99; S, 48.19. IR (KBr; cm^{-1}): (C−H) 2951, 2864; (C═C) 1455, 1381; (C═S) 1080, 960.

Electrocrystallization of $(Bu_4N)_x\{tto[Ni(dmit)]_2\}$. A black, microcrystalline and brittle material was obtained by constant current electrolysis of a CH_3CN/DMF (4:1) solution containing 0.01 M Bu_4NBr and saturated with $(Bu_4N)_2\{tto[Ni(dmit)]_2\}$ (**1**). A glass, two-compartment H-cell separated by a medium-porosity frit was used similar to that previously described in ref 2f. Pt wire (0.5 mm diameter) was used for the electrodes, and the cell was flushed with argon. A current density of 0.5 μA/cm^2 was applied over a period of 45 days at room temperature. The microcrystalline material was harvested from the anode, washed thoroughly with methanol followed by diethyl ether, and dried under vacuum.

Synthesis of $(TTF)_{0.57}\{tto[Ni(dmit)]_2\}$. A black-brown precipitate of approximate stoichiometry $(TTF)_{0.57}\{tto[Ni(dmit)]_2\}$ was obtained by slow interdiffusion of saturated solutions of $(TTF)_3(BF_4)_2$[12] and $(Bu_4N)_2\{tto[Ni(dmit)]_2\}$ in CH_3CN under an argon atmosphere at room temperature. A three-compartment glass cell separated by course-porosity frits was used similar to that described in ref 4a. The precipitate was isolated after 60 days, washed with acetone, followed by methanol and diethyl ether, and dried under vacuum. Anal. Calcd for $C_{74}H_{28}S_{84}Ni_8$: C, 21.79; H, 0.70; N, 0.00. Found: C, 21.92; H, 0.98; N, <0.02.

Chemical Oxidation of $(Bu_4N)_2\{tto[Ni(dmit)]_2\}$ (1). A black precipitate of approximate stoichiometry $(Bu_4N)_{0.33}\{tto[Ni(dmit)]_2\}$ was obtained from the rapid mixing of solutions of 3 mg (0.1 mmol) of I_2 and 2 mg (0.1 mmol) of NaI with 100 mg (0.090 mmol) of $(Bu_4N)_2\{tto[Ni(dmit)]_2\}$ (**1**) in acetone. A black precipitate was filtered, washed with acetone, followed by methanol and diethyl ether, and dried under vacuum. Anal. Calcd for $C_{40}H_{36}NS_{42}Ni_6$: C, 21.55; H, 1.63; N, 0.63; S, 60.40. Found: C, 21.23; H, 1.58; N, 0.60; S, 60.00.

X-ray Structure Determinations. Crystallographic data for $(Bu_4N)_2\{tto[Ni(dsit)]_2\}$ (**2**), $(Bu_4N)_2\{tto[Ni(dmise)]_2\}$ (**3**), $(Me_4N)_2\{tto[Ni(dmit)]_2\}$ (**4**), and $(Et_4N)_2\{tto[Ni(dmit)]_2\}$ (**5**) are listed in Table 1. Data were collected at 173 K on a Siemens SMART PLATFORM equipped with a CCD area detector. For complexes **2** and **3**, crystals suitable for X-ray studies were obtained by slow evaporation of a concentrated solution of the complexes in DMF. For **2**, dark brown-black rectangular-shaped crystals (0.48 × 0.16 × 0.07 mm^3) were chosen for study; for **3**, dark brown-black block-like crystals (0.48 × 0.23 × 0.17 mm^3) were chosen; for **4**, black chunk-like crystals (0.32 × 0.21 × 0.07 mm^3) were chosen; and for **5**, black chunk-like crystals (0.44 × 0.23 × 0.20 mm^3) were chosen for study.

The diffractometer was equipped with a graphite monochromator utilizing Mo Kα radiation (λ = 0.710 73 Å). Cell parameters were refined using up to 8192 reflections. A hemisphere of data (1381 frames) was collected using the ω-scan method (0.3° frame width). The first 50 frames were remeasured at the end of data collection to monitor instrument and crystal stability (maximum correction on I was <1%). ψ-scan absorption corrections were applied based on the entire data set. The structures were solved by the direct methods in SHELXTL and refined using full matrix least squares. The non-H atoms were treated anisotropically, whereas the hydrogen atoms were calculated in ideal positions and were riding on their respective carbon atoms except in $(Et_4N)_2\{tto[Ni(dmit)]_2\}$ (**5**), where all of the H atoms were refined without any constraints. All refinements were done using F^2.

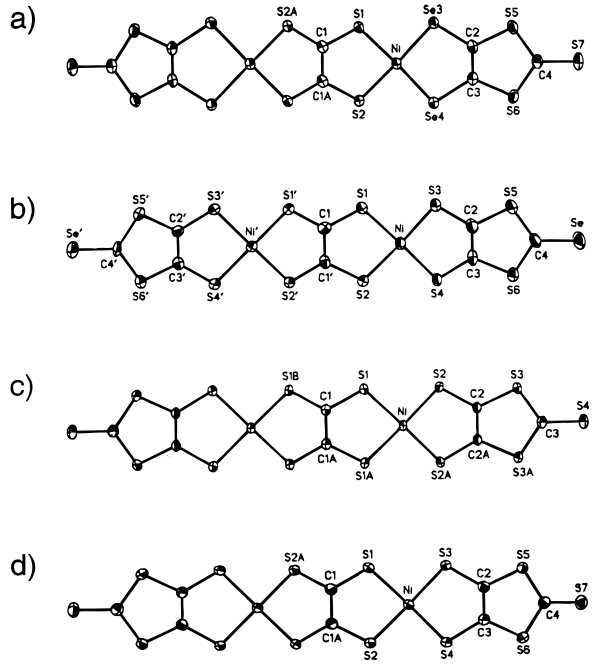

Figure 1. Thermal ellipsoid drawings (50% probability) and numbering schemes for the dianions of (a) $(Bu_4N)_2\{tto[Ni(dsit)]_2\}$ (**2**), (b) $(Bu_4N)_2\{tto[Ni(dmise)]_2\}$ (**3**), (c) $(Me_4N)_2\{tto[Ni(dmit)]_2\}$ (**4**), and (d) $(Et_4N)_2\{tto[Ni(dmit)]_2\}$ (**5**).

Molecular numbering schemes for the dianion of $(Bu_4N)_2\{tto[Ni(dsit)]_2\}$ (**2**), $(Bu_4N)_2\{tto[Ni(dmise)]_2\}$ (**3**), $(Me_4N)_2\{tto[Ni(dmit)]_2\}$ (**4**), and $(Et_4N)_2\{tto[Ni(dmit)]_2\}$ (**5**) are shown in Figure 1. Atomic coordinates and their estimated standard deviations are collected for **2** in Table 2, for **3** in Table 3, for **4** in Table 4, and for **5** in Table 5. Selected bond lengths and angles can be found for $(Bu_4N)_2\{tto[Ni(dsit)]_2\}$ (**2**) in Table 6, for $(Bu_4N)_2\{tto[Ni(dmise)]_2\}$ (**3**) in Table 7, for $(Me_4N)_2\{tto[Ni(dmit)]_2\}$ (**4**) in Table 8, and for $(Et_4N)_2\{tto[Ni(dmit)]_2\}$ (**5**) in Table 9.

Electrochemical Methods. Cyclic voltammetry was performed on an EG&G Princeton Applied Research 273 potentiostat utilizing Model 270/250 Electrochemistry Software 4.23 (Copyright 1995 EG&G Instruments Inc.). Acetonitrile was dried and distilled over CaH_2 and thoroughly degassed with argon prior to use. Tetramethylammonium

(12) Wudl, F. *J. Am. Chem. Soc.* **1975**, *97*, 1962.

Table 2. Atomic Coordinates ($\times 10^4$) and Equivalent Isotropic[a] Displacement Parameters ($Å^2 \times 10^3$) for the Non-H Atoms of $(Bu_4N)_2\{tto[Ni(dsit)]_2\}$ (**2**)

atom	*x*	*y*	*z*	U_{eq}
Ni	3933(1)	10060(1)	1553(1)	20(1)
Se(3)	1797(1)	9865(1)	1994(1)	23(1)
Se(4)	4951(1)	9950(1)	2700(1)	26(1)
S(1)	3029(1)	10211(1)	452(1)	26(1)
S(2)	5939(1)	10086(1)	1084(1)	24(1)
S(5)	880(1)	9492(1)	3653(1)	28(1)
S(6)	3588(1)	9546(1)	4267(1)	29(1)
S(7)	1286(1)	9192(1)	5293(1)	36(1)
C(1)	4321(3)	10030(2)	−149(2)	21(1)
C(2)	2177(3)	9693(2)	3022(2)	23(1)
C(3)	3434(3)	9719(2)	3305(2)	23(1)
C(4)	1882(3)	9392(2)	4454(2)	26(1)
N(1)	1717(2)	12600(1)	3194(1)	21(1)
C(11)	2235(3)	13035(2)	2490(2)	24(1)
C(12)	2713(3)	12419(2)	1879(2)	31(1)
C(13)	3433(3)	12904(2)	1253(2)	32(1)
C(14)	2593(4)	13614(2)	889(2)	42(1)
C(21)	2834(3)	12081(2)	3581(2)	26(1)
C(22)	4036(3)	12620(2)	3840(2)	34(1)
C(23)	5128(3)	12073(2)	4214(2)	33(1)
C(24)	6260(4)	12644(2)	4527(2)	48(1)
C(31)	1224(3)	13327(2)	3702(2)	22(1)
C(32)	756(3)	13045(2)	4474(2)	28(1)
C(33)	−190(3)	13727(2)	4788(2)	31(1)
C(34)	−600(4)	13545(3)	5587(2)	42(1)
C(41)	565(3)	11974(2)	3012(2)	24(1)
C(42)	−660(3)	12385(2)	2634(2)	31(1)
C(43)	−1827(3)	11748(2)	2545(2)	33(1)
C(44)	−3052(3)	12188(2)	2178(2)	41(1)

[a] $U_{eq} = (1/3)\sum_i\sum_j U_{ij}a_i^*a_j^*A_{ij}$ where A_{ij} is the dot product of the *i*th and *j*th direct-space unit cell vectors.

perchlorate (TMAP) was used as supporting electrolyte (0.05 M). Ag/Ag^+ was used as the reference electrode with a Pt button working electrode and Pt foil counter electrode. Electrochemistry was completed under an argon atmosphere. Saturated solutions of the complexes were used in the cyclic voltammetry experiments.

Conductivity Measurements. Conductivity data was obtained using a two-probe pressed-powder method with contacts made using fast-drying gold paint (Ted Pella). A Keithley 169 multimeter was used to measure sample resistances.

Results and Discussion

Synthesis of $(Bu_4N)_2\{tto[Ni(dsit)]_2\}$ (2), $(Bu_4N)_2\{tto[Ni(dmise)]_2\}$ (3), $(Me_4N)_2\{tto[Ni(dmit)]_2\}$ (4), and $(Et_4N)_2\{tto[Ni(dmit)]_2\}$ (5). In order to prepare the bimetallic, tetrathiooxalato-bridged Ni(II) complexes **1**−**5** similar to the previously reported Cu(II) bimetallic complexes **6**−**9**,[7] a new synthetic methodology was developed. The synthetic method used to assemble **6**−**9** could not be used to synthesize the Ni(II) analogs due to the fact that the rate of metal exchange with Zn(II) is much slower than the reaction with tto^{2-}. This resulted primarily in the formation of $[Ni(tto)]_n$ oligomer. The new method is also based on competing reactions but with a slight variation. A solution of $NiCl_2{\cdot}6H_2O$ in methanol was added to a stirring acetone solution containing Bu_4NBr, $(Et_4N)_2tto$, and the dicesium salt of the capping ligand of choice. The tto salt is only slightly soluble in acetone and gradually dissolved, allowing it to simultaneously react with Ni(II) along with the dithiolato capping ligands over a period of approximately 1 h. Once the reaction was complete, the solution was filtered to remove undissolved $(Et_4N)_2tto$ and $[Ni(tto)]_n$, a black insoluble oligomer. An equivalent amount of 2-propanol was added to the solution and allowed to evaporate to less than half overnight. The lesser soluble bimetallic complexes crystallized out and were separated. The synthetic procedures are readily reproducible for $(Bu_4N)_2\{tto[Ni(dmit)]_2\}$ (**1**) in 41%, $(Bu_4N)_2\{tto[Ni(dsit)]_2\}$ (**2**) in 41%, and $(Bu_4N)_2\{tto[Ni(dmise)]_2\}$ (**3**) in 32% yield. This synthetic method is different from the recently reported synthesis of the analogous Cu(II) bimetallic complexes which employed a three-solvent biphasic system.[7] The synthesis also depends on competing reactions where thiophilic Cu(II) ion metal exchanges with the Zn(II) bis-chelate ($[Zn(L)_2]^{2-}$) of the ligand of choice in the organic layer, and also reacts with

Table 3. Atomic Coordinates ($\times 10^4$) and Equivalent Isotropic[a] Displacement Parameters ($Å^2 \times 10^3$) for the Non-H Atoms of $(Bu_4N)_2\{tto[Ni(dmise)]_2\}$ (**3**)

atom	*x*	*y*	*z*	U_{eq}
Ni′	5238(1)	4974(1)	1034(1)	23(1)
Ni	4769(1)	5053(1)	−711(1)	27(1)
Se	4133(1)	5252(1)	−2821(1)	52(1)
Se′	5898(1)	4706(1)	3146(1)	46(1)
S(1′)	3774(1)	4509(1)	619(1)	27(1)
S(1)	3592(1)	4506(1)	−248(1)	6(1)
C(1′)	5621(5)	5246(3)	152(1)	24(1)
C(1)	4386(5)	4775(3)	174(1)	24(1)
S(2)	6212(1)	5553(1)	−295(1)	28(1)
S(2′)	6472(1)	5482(1)	569(1)	26(1)
C(2′)	4882(5)	4680(3)	1905(1)	25(1)
C(2)	3928(5)	4899(3)	−1559(2)	33(1)
S(3)	3288(2)	4553(1)	−1115(1)	42(1)
S(3′)	3929(1)	4495(1)	1488(1)	25(1)
C(3)	5093(5)	5348(3)	−1580(1)	29(1)
C(3′)	6128(5)	5058(3)	1881(1)	28(1)
S(4)	6017(1)	5582(1)	−1166(1)	26(1)
S(4′)	6773(1)	5392(1)	1443(1)	31(1)
C(4′)	5751(6)	4764(3)	2619(1)	30(1)
C(4)	4262(6)	5209(4)	−2295(2)	34(1)
S(5′)	4350(1)	4401(1)	2372(1)	32(1)
S(5)	3105(2)	4708(1)	−2002(1)	44(1)
S(6)	5593(1)	5645(1)	−2047(1)	3(1)
S(6′)	6974(1)	5183(1)	2324(1)	32(1)
N(1)	1224(4)	6747(2)	1193(1)	25(1)
C(11)	25(5)	7217(3)	1018(2)	29(1)
C(12)	−1155(5)	7414(3)	1295(2)	34(1)
C(13)	−2309(6)	7820(4)	1066(2)	42(1)
C(14)	−3439(6)	8098(5)	1330(2)	60(2)
C(21)	808(6)	5876(3)	1309(2)	29(1)
C(22)	261(5)	5322(3)	988(2)	29(1)
C(23)	70(6)	4449(3)	1142(2)	34(1)
C(24)	−505(7)	3871(4)	836(2)	51(2)
C(31)	2346(6)	6702(3)	884(2)	32(1)
C(32)	3043(6)	7511(3)	791(2)	38(1)
C(33)	4086(7)	7384(4)	463(2)	48(2)
C(34)	3490(9)	7237(5)	71(2)	69(2)
C(41)	1724(6)	7188(3)	1555(2)	32(1)
C(42)	3006(6)	6838(3)	1741(2)	37(1)
C(43)	3411(8)	7340(4)	2094(2)	60(2)
C(44)	4659(7)	6999(4)	2291(2)	57(2)
N(2)	3567(5)	1755(3)	1030(2)	37(1)
C(51)	2584(6)	1669(4)	1365(2)	42(2)
C(52)	2038(8)	2481(4)	1523(2)	61(2)
C(53)	922(10)	2335(6)	1820(3)	87(3)
C(54)	1368(14)	1957(7)	2165(3)	141(6)
C(61)	4827(7)	2247(4)	1142(2)	53(2)
C(62)	5528(7)	2053(6)	1511(2)	86(3)
C(63)	6751(10)	2684(7)	1491(3)	55(3)
C(64)	7344(13)	2848(8)	1912(3)	73(4)
C(63′)	7039(13)	2166(12)	1658(8)	76(8)
C(64′)	7078(31)	3140(12)	1638(9)	89(9)
C(71)	2962(7)	2206(3)	685(2)	46(2)
C(72)	1616(6)	1857(4)	531(2)	46(2)
C(73)	1245(9)	2278(5)	149(2)	66(2)
C(74)	2062(7)	2004(4)	−195(2)	59(2)
C(81)	3965(6)	870(3)	921(2)	34(1)
C(82)	4633(6)	733(3)	528(2)	36(1)
C(83)	4998(5)	−195(3)	492(2)	35(1)
C(84)	5244(7)	−427(4)	69(2)	51(2)

[a] $U_{eq} = (1/3)\sum_i\sum_j U_{ij}a_i^*a_j^*A_{ij}$ where A_{ij} is the dot product of the *i*th and *j*th direct-space unit cell vectors.

Table 4. Atomic Coordinates ($\times 10^4$) and Equivalent Isotropic[a] Displacement Parameters ($Å^2 \times 10^3$) for the Non-H Atoms of $(Me_4N)_2\{tto[Ni(dmit)]_2\}$ (**4**)

atom	*x*	*y*	*z*	U_{eq}
Ni	8217(1)	−5000	17459(1)	19(1)
S(1)	9108(1)	−6528(1)	18745(1)	24(1)
S(2)	7361(1)	−6559(1)	16181(1)	23(1)
S(3)	5443(1)	−6432(1)	13683(1)	22(1)
S(4)	3793(1)	−5000	11553(1)	35(1)
C(1)	10000	−5707(3)	20000	18(1)
C(2)	6431(1)	−5673(2)	14972(2)	18(1)
C(3)	4835(2)	−5000	12906(3)	21(1)
N	1898(2)	−5000	7838(2)	25(1)
C(4)	3006(3)	−5000	7918(4)	43(1)
C(5)	1098(4)	−5000	6526(4)	58(1)
C(6)	1744(2)	−3780(2)	8450(2)	33(1)

[a] $U_{eq} = (1/3)\sum_i\sum_j U_{ij} a_i^* a_j^* A_{ij}$ where A_{ij} is the dot product of the *i*th and *j*th direct-space unit cell vectors.

Table 5. Atomic Coordinates ($\times 10^4$) and Equivalent Isotropic[a] Displacement Parameters ($Å^2 \times 10^3$) for the Non-H Atoms of $(Et_4N)_2\{tto[Ni(dmit)]_2\}$ (**5**)

atom	*x*	*y*	*z*	U_{eq}
Ni	3919(1)	−5149(1)	6493(1)	20(1)
S(1)	4099(1)	−3717(1)	5585(1)	24(1)
S(2)	4633(1)	−6469(1)	5780(1)	24(1)
S(3)	3263(1)	−3799(1)	7227(1)	24(1)
S(4)	3897(1)	−6589(1)	7443(1)	24(1)
S(5)	2994(1)	−3934(1)	9142(1)	25(1)
S(6)	3567(1)	−6492(1)	9327(1)	26(1)
S(7)	3257(1)	−5187(1)	10934(1)	33(1)
C(1)	4881(2)	−4360(2)	4957(1)	20(1)
C(2)	3263(2)	−4611(2)	8197(1)	22(1)
C(3)	3530(2)	−5812(2)	8286(1)	22(1)
C(4)	3282(2)	−5202(2)	9859(1)	24(1)
N	−818(1)	−5524(2)	7129(1)	19(1)
C(11)	−2068(2)	−5716(2)	7171(2)	26(1)
C(12)	−2311(2)	−6981(3)	7433(2)	40(1)
C(13)	158(2)	−5903(2)	8044(1)	23(1)
C(14)	48(2)	−5361(2)	8920(2)	31(1)
C(15)	−705(2)	−6296(2)	6342(2)	25(1)
C(16)	442(2)	−6092(2)	6137(2)	30(1)
C(17)	−647(2)	−4188(2)	6970(1)	24(1)
C(18)	−1498(2)	−3679(2)	6052(2)	35(1)

[a] $U_{eq} = (1/3)\sum_i\sum_j U_{ij} a_i^* a_j^* A_{ij}$ where A_{ij} is the dot product of the *i*th and *j*th direct-space unit cell vectors.

tto at the interface of the aqueous and organic layers to assemble the bimetallic complexes. Other products formed are insoluble oligomeric $[Cu(tto)]_n$ and the bis-chelate $[Cu(L)_2]^{2-}$. Yields for the Cu(II) bimetallic complexes synthesized range from only 14 to 25%.[7]

The compounds $(Me_4N)_2\{tto[Ni(dmit)]_2\}$ (**4**) and $(Et_4N)_2\{tto[Ni(dmit)]_2\}$ (**5**) with smaller cations were synthesized from $(Bu_4N)_2\{tto[Ni(dmit)]_2\}$ (**1**) via cation exchange reactions. The resulting Me_4N^+ (**4**) and Et_4N^+ (**5**) salts are less soluble than **1** and were crystallized from solutions of $(Bu_4N)_2\{tto[Ni(dmit)]_2\}$ (**1**) in the presence of an excess of Me_4NClO_4 and Et_4NBr electrolytes, respectively. $(Me_4N)_2\{tto[Ni(dmit)]_2\}$ (**4**) and $(Et_4N)_2\{tto[Ni(dmit)]_2\}$ (**5**) were both prepared in 8% yield.

Crystal and Molecular Structures of Complexes 1−5. The structure of $(Bu_4N)_2\{tto[Ni(dmit)]_2\}$ (**1**) has been previously reported[8] and will be discussed alongside complexes $(Bu_4N)_2\{tto[Ni(dsit)]_2\}$ (**2**), $(Bu_4N)_2\{tto[Ni(dmise)]_2\}$ (**3**), $(Me_4N)_2\{tto[Ni(dmit)]_2\}$ (**4**), and $(Et_4N)_2\{tto[Ni(dmit)]_2\}$ (**5**). As can be seen in Figure 1, all of the complexes are composed of Ni(II) metal centers bridged by the side-on coordination of the tto ligand and capped by the dithiolato ligand of dmit for **1**, **4**, and **5**, dsit for **2** and the dmise ligand for complex **3**. The Ni(II) bimetallic complexes presented here have values in the narrow range of 1.416(7) Å for **1** to 1.444(5) Å for complex **2**. It is interesting to note that there is a difference in this bond length between complex **1** (1.416(7) Å) and complexes **4** and **5** (1.430(6) and 1.434(4) Å, respectively) simply due to a change of cation. From the crystal structure of $[(Ph_3P)_2Cu]_2(C_2S_4)$ reported by Hansen et al., the tto ligand, which is also side-on coordinated, has a carbon−carbon bond length of 1.53(8) Å[13]

Table 6. Selected Bond Lengths (Å) and Angles (deg) for the Dianion of $(Bu_4N)_2\{tto[Ni(dsit)]_2\}$ (**2**)

Ni−S(2)	2.1617(7)	S(5)−C(4)	1.741(3)
Ni−S(1)	2.1663(7)	S(5)−C(2)	1.744(3)
Ni−Se(3)	2.2821(4)	S(6)−C(4)	1.739(3)
Ni−Se(4)	2.2840(4)	S(6)−C(3)	1.746(3)
Se(3)−C(2)	1.890(3)	S(7)−C(4)	1.646(3)
Se(4)−C(3)	1.891(3)	C(1)−C(1)#1[a]	1.444(5)
S(1)−C(1)	1.700(3)	C(1)−S(2)#1	1.699(3)
S(2)−C(1)#1	1.699(3)	C(2)−C(3)	1.338(4)
S(2)−Ni−S(1)	91.05(3)	C(1)#1−C(1)−S(2)#1	119.2(3)
S(2)−Ni−Se(3)	173.07(3)	C(1)#1−C(1)−S(1)	118.7(3)
S(1)−Ni−Se(3)	87.34(2)	S(2)#1−C(1)−S(1)	122.1(2)
S(2)−Ni−Se(4)	87.19(2)	C(3)−C(2)−S(5)	116.5(2)
S(1)−Ni−Se(4)	177.48(3)	C(3)−C(2)−Se(3)	122.6(2)
Se(3)−Ni−Se(4)	94.62(2)	S(5)−C(2)−Se(3)	120.9(2)
C(2)−Se(3)−Ni	100.30(9)	C(2)−C(3)−S(6)	116.1(2)
C(3)−Se(4)−Ni	100.49(8)	C(2)−C(3)−Se(4)	121.9(2)
C(1)−S(1)−Ni	104.54(9)	S(6)−C(3)−Se(4)	122.0(2)
C(1)#1−S(2)−Ni	104.40(10)	S(7)−C(4)−S(6)	123.9(2)
C(4)−S(5)−C(2)	97.58(14)	S(7)−C(4)−S(5)	124.1(2)
C(4)−S(6)−C(3)	97.76(13)	S(6)−C(4)−S(5)	112.0(2)

[a] Symmetry transformations used to generate equivalent atoms: #1 $-x+1, -y+2, -z$.

Table 7. Selected Bond Lengths (Å) and Angles (deg) for the Dianion of $(Bu_4N)_2\{tto[Ni(dmise)]_2\}$ (**3**)

Ni′−S(1′)	2.1595(14)	C(2′)−C(3′)	1.371(7)
Ni′−S(3′)	2.1633(14)	C(2′)−S(3′)	1.735(5)
Ni′−S(2′)	2.1643(14)	C(2′)−S(5′)	1.747(5)
Ni′−S(4′)	2.168(2)	C(2)−C(3)	1.358(8)
Ni−S(1)	2.156(2)	C(2)−S(3)	1.741(5)
Ni−S(4)	2.1617(14)	C(2)−S(5)	1.746(5)
Ni−S(3)	2.167(2)	C(3)−S(4)	1.729(5)
Ni−S(2)	2.1677(14)	C(3)−S(6)	1.743(5)
Se−C(4)	1.812(5)	C(3′)−S(4′)	1.720(5)
Se′−C(4′)	1.817(5)	C(3′)−S(6′)	1.744(5)
S(1′)−C(1)	1.696(5)	C(4′)−S(6′)	1.711(5)
S(1)−C(1)	1.699(5)	C(4′)−S(5′)	1.719(6)
C(1′)−C(1)	1.435(6)	C(4)−S(6)	1.712(5)
C(1′)−S(2′)	1.700(5)	C(4)−S(5)	1.721(6)
C(1′)−S(2)	1.714(5)		
S(1′)−Ni′−S(3′)	87.35(5)	S(3′)−C(2′)−S(5′)	123.4(3)
S(1′)−Ni′−S(2′)	91.17(5)	C(3)−C(2)−S(3)	121.5(4)
S(3′)−Ni′−S(2′)	177.49(6)	C(3)−C(2)−S(5)	116.1(4)
S(1′)−Ni′−S(4′)	177.25(6)	S(3)−C(2)−S(5)	122.4(3)
S(3′)−Ni′−S(4′)	93.43(5)	C(2)−S(3)−Ni	101.4(2)
S(2′)−Ni′−S(4′)	88.15(5)	C(2′)−S(3′)−Ni′	102.2(2)
S(1)−Ni−S(4)	177.86(6)	C(2)−C(3)−S(4)	121.2(4)
S(1)−Ni−S(3)	87.62(6)	C(2)−C(3)−S(6)	115.7(4)
S(4)−Ni−S(3)	93.84(6)	S(4)−C(3)−S(6)	123.2(3)
S(1)−Ni−S(2)	91.10(5)	C(2′)−C(3′)−S(4′)	121.4(4)
S(4)−Ni−S(2)	87.46(5)	C(2′)−C(3′)−S(6′)	115.3(4)
S(3)−Ni−S(2)	178.58(6)	S(4′)−C(3′)−S(6′)	123.4(3)
C(1)−S(1′)−Ni′	105.6(2)	C(3)−S(4)−Ni	102.0(2)
C(1)−S(1)−Ni	106.0(2)	C(3′)−S(4′)−Ni′	102.2(2)
C(1)−C(1′)−S(2′)	119.5(3)	S(6′)−C(4′)−S(5′)	114.1(3)
C(1)−C(1′)−S(2)	119.1(3)	S(6′)−C(4′)−Se′	123.6(3)
S(2′)−C(1′)−S(2)	121.5(3)	S(5′)−C(4′)−Se′	122.3(3)
C(1′)−C(1)−S(1′)	118.7(3)	S(6)−C(4)−S(5)	114.1(3)
C(1′)−C(1)−S(1)	118.8(3)	S(6)−C(4)−Se	122.2(3)
S(1′)−C(1)−S(1)	122.5(3)	S(5)−C(4)−Se	123.7(3)
C(1′)−S(2)−Ni	105.1(2)	C(4′)−S(5′)−C(2′)	97.1(2)
C(1′)−S(2′)−Ni′	105.0(2)	C(4)−S(5)−C(2)	96.8(3)
C(3′)−C(2′)−S(3′)	120.7(4)	C(4)−S(6)−C(3)	97.3(3)
C(3′)−C(2′)−S(5′)	115.9(4)	C(4′)−S(6′)−C(3′)	97.7(2)

Table 8. Selected Bond Lengths (Å) and Angles (deg) for the Dianion of $(Me_4N)_2\{tto[Ni(dmit)]_2\}$ (**4**)

Ni−S(1)#1	2.1616(5)	S(3)−C(2)	1.748(2)
Ni−S(1)	2.1617(5)	S(4)−C(3)	1.651(3)
Ni−S(2)#1	2.1674(5)	C(1)−C(1)#2	1.430(6)
Ni−S(2)	2.1675(5)	C(1)−S(1)#3	1.704(2)
S(1)−C(1)	1.704(2)	C(2)−C(2)#1	1.361(4)
S(2)−C(2)	1.726(2)	C(3)−S(3)#1	1.733(2)
S(3)−C(3)	1.733(2)		
S(1)#1−Ni−S(1)	91.19(3)	C(1)#2−C(1)−S(1)	119.13(9)
S(1)#1−Ni−S(2)#1	87.75(2)	C(1)#2−C(1)−S(1)#3	119.13(9)
S(1)−Ni−S(2)#1	178.52(2)	S(1)−C(1)−S(1)#3	121.7(2)
S(1)#1−Ni−S(2)	178.52(2)	C(2)#1−C(2)−S(2)	121.25(7)
S(1)−Ni−S(2)	87.75(2)	C(2)#1−C(2)−S(3)	116.01(7)
S(2)#1−Ni−S(2)	93.28(3)	S(2)−C(2)−S(3)	122.74(12)
C(1)−S(1)−Ni	105.27(9)	S(4)−C(3)−S(3)#1	123.39(8)
C(2)−S(2)−Ni	101.92(7)	S(4)−C(3)−S(3)	123.39(8)
C(3)−S(3)−C(2)	97.37(11)	S(3)#1−C(3)−S(3)	113.2(2)

[a] Symmetry transformations used to generate equivalent atoms: #1 $x, -y-1, z$; #2 $-x+2, -y-1, -z+4$; #3 $-x+2, y, -z+4$.

Table 9. Selected Bond Lengths (Å) and Angles (deg) for the Dianion of $(Et_4N)_2\{tto[Ni(dmit)]_2\}$ (**5**)

Ni−S(4)	2.1585(5)	S(5)−C(4)	1.734(2)
Ni−S(1)	2.1625(5)	S(5)−C(2)	1.754(2)
Ni−S(2)	2.1633(5)	S(6)−C(4)	1.730(2)
Ni−S(3)	2.1680(5)	S(6)−C(3)	1.747(2)
S(1)−C(1)	1.709(2)	S(7)−C(4)	1.655(2)
S(2)−C(1)#1	1.702(2)	C(1)−C(1)#1	1.434(4)
S(3)−C(2)	1.733(2)	C(1)−S(2)#1	1.702(2)
S(4)−C(3)	1.728(2)	C(2)−C(3)	1.356(3)
S(4)−Ni−S(1)	175.34(2)	C(1)#1−C(1)−S(2)#1	119.2(2)
S(4)−Ni−S(2)	86.94(2)	C(1)#1−C(1)−S(1)	118.9(2)
S(1)−Ni−S(2)	91.18(2)	S(2)#1−C(1)−S(1)	121.90(12)
S(4)−Ni−S(3)	93.57(2)	C(3)−C(2)−S(3)	121.2(2)
S(1)−Ni−S(3)	88.17(2)	C(3)−C(2)−S(5)	115.9(2)
S(2)−Ni−S(3)	178.07(2)	S(3)−C(2)−S(5)	122.84(12)
C(1)−S(1)−Ni	104.84(7)	C(2)−C(3)−S(4)	121.4(2)
C(1)#1−S(2)−Ni	104.96(7)	C(2)−C(3)−S(6)	116.01(14)
C(2)−S(3)−Ni	101.52(7)	S(4)−C(3)−S(6)	122.49(12)
C(3)−S(4)−Ni	101.85(7)	S(7)−C(4)−S(6)	123.49(12)
C(4)−S(5)−C(2)	97.27(10)	S(7)−C(4)−S(5)	123.46(12)
C(4)−S(6)−C(3)	97.56(10)	S(6)−C(4)−S(5)	113.04(11)

[a] Symmetry transformations used to generate equivalent atoms: #1 $-x+1, -y-1, -z+1$.

where the core is made up of a planar Cu−tto−Cu unit. This value is better for comparison to our compounds than the value reported from the crystal structure of $(Et_4N)_2$tto, where the S−C−S components of the uncoordinated tto ligand are in a staggered formation with respect to each other. The values reported are similar, though, with the value of 1.516(6) Å[14] for $(Et_4N)_2$tto. In the Cu(II) bimetallic complexes previously reported, the lengths of the central carbon−carbon bond of tto are longer, with $(Bu_4N)_2\{tto[Cu(mnt)]_2\}$ being the longest at 1.483(9) Å[7b] and $(Ph_4As)_2\{tto[Cu(dmid)]_2\}$ having the shortest bond length of 1.467(1) Å.[15] In the complex $Ni_2(\eta^5\text{-}C_5Me_5)_2(C_2S_4)$ reported by Dahl and co-workers,[5] this complex also possesses a planar Ni−C_2S_4−Ni core where the C−C bond of the bridging tto ligand was reported to be 1.360(11) Å, which is similar in length to the ett (ett = ethylenetetrathiolate = $C_2S_4^{4-}$) ligand.[16] The complex $(Et_4N)_2[Ni_2C_2S_4\{S_2C_2S_2C_2(CO_2Me)_2\}_2]$ reported in 1994 by Rauchfuss and co-workers has a value of 1.43 Å for the C−C bond of the side-on coordinated tto ligand which is very similar to that of the central C−C bond of the C_2S_4 ligand of the complexes **1**−**5**. This approximate length was interpreted to be an intermediate between the central C_2S_4 ligand acting as tto and ett.[6]

Table 10. Values of the Dihedral Angles (deg) Formed between the Plane of the Bridging tto Ligand (**Y**) and the Capping dmit Ligands (**X** and **Z**) (L(**X**)−Ni′−tto(**Y**)−Ni−L(**Z**))

complex	Θ	Φ
$(Bu_4N)_2\{tto[Ni(dmit)]_2\}$ (**1**)	5.7	2.0[a]
$(Bu_4N)_2\{tto[Ni(dsit)]_2\}$ (**2**)	20.5	20.5[b]
$(Bu_4N)_2\{tto[Ni(dmise)]_2\}$ (**3**)	6.1	2.3[a]
$(Me_4N)_2\{tto[Ni(dmit)]_2\}$ (**4**)	3.6	3.6[b]
$(Et_4N)_2\{tto[Ni(dmit)]_2\}$ (**5**)	24.5	24.5[b]

[a] Crystallographically independent. [b] Equal by symmetry.

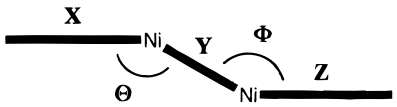

Figure 2. Conceptual drawing showing the dihedral angles formed in complexes $(Bu_4N)_2\{tto[Ni(dmit)]_2\}$ (**1**), $(Bu_4N)_2\{tto[Ni(dsit)]_2\}$ (**2**), $(Bu_4N)_2\{tto[Ni(dmise)]_2\}$ (**3**), $(Me_4N)_2\{tto[Ni(dmit)]_2\}$ (**4**), and $(Et_4N)_2\{tto[Ni(dmit)]_2\}$ (**5**).

The Ni(C_2S_4)Ni core of each complex is planar and extensively delocalized. For complexes **1**−**5**, all Ni−S distances to the tto ligand are between 2.1595(14) and 2.1677(14) Å. These bond lengths are essentially the same, indicating a highly conjugated Ni(C_2S_4)Ni core. This is seen in the previously reported similar Cu(II) bimetallic complexes.[7]

The coordination about the d^8 Ni(II) metal centers is square planar as expected. Examining the S−Ni−S bond angles with the tto bridging ligand, the values are very close to 90°: between 91.05(3)° for $(Bu_4N)_2\{tto[Ni(dsit)]_2\}$ (**2**) and 91.35(7)° for $(Bu_4N)_2\{tto[Ni(dmit)]_2\}$ (**1**). The S−Ni−S bond angles with the capping ligands and the Se−Ni−Se bond angles for **2** range from 93.28(3)° for $(Me_4N)_2\{tto[Ni(dmit)]_2\}$ (**4**) to 94.62(2)° for $(Bu_4N)_2\{tto[Ni(dsit)]_2\}$ (**2**). The complexes are not perfectly planar but have dihedral angles formed between the planes of the bridging tto and capping ligands. The values of the dihedral angles for **1**−**5** are listed in Table 10. In the Cu(II) bimetallic complexes, a dihedral angle was formed between the same ligand planes due to a twist at the metal center as a result of a tetrahedral distortion from square planarity.[7] $\{tto[Cu(dmid)]_2\}^{2-}$ had the highest dihedral angle of 28.3°, with $(Bu_4N)_2\{tto[Cu(mnt)]_2\}$ (**7**) being the only completely planar bimetallic Cu(II) complex with a dihedral angle of 0°.[7b,15b] In the Ni(II) bimetallic complexes presented, dihedral angles are not a result of a tetrahedral distortion but rather a hinge-like bend at the thiolate atoms of complexes **3**−**5** and selenolate atoms of **2**. This is illustrated in the conceptual drawing in Figure 2 where Θ and Φ represent dihedral angles between planes $X-Y$ and $Y-Z$, respectively. The complex $(Bu_4N)_2\{tto[Ni(dmise)]_2\}$ (**3**) has the smallest dihedral angle of 2.3°, with $(Et_4N)_2\{tto[Ni(dmit)]_2\}$ (**5**) having the largest dihedral angle of 24.5°. It is interesting to note that in complexes **1**, **4**, and **5** where the dianion $\{tto[Ni(dmit)]_2\}^{2-}$ is the same, there are large differences in the dihedral angles found in the crystal structure as a result of changing the cation and the resulting change in the intermolecular interactions. In **1**, the large Bu_4N^+ cation induces the formation of dihedral angles of 2.0° and 5.7° for the crystallographically independent halves of the dianion. In **4** with the Me_4N^+ cation, the dihedral angle is only 3.6°, while in complex

(13) Hansen, L. K.; Sieler, J.; Strauch, P.; Dietzsch, W.; Hoyer, E. *Acta Chem. Scand. Ser. A* **1985**, *39*, 571.
(14) Bacher, A. D.; Sens, I.; Müller, U. *Z. Naturforsch.* **1992**, *47b*, 702.
(15) (a) Vicente, R.; Ribas, J.; Cassoux, P.; Valade, L. *Synth. Met.* **1986**, *13*, 265. (b) Vicente, R.; Ribas, J.; Alvarez, S.; Segui, A.; Solans, X.; Verdaguer, M. *Inorg. Chem.* **1987**, *26*, 4004.
(16) Dietzsch, W.; Strauch, P.; Hoyer, E. *Coord. Chem. Rev.* **1992**, *121*, 43.

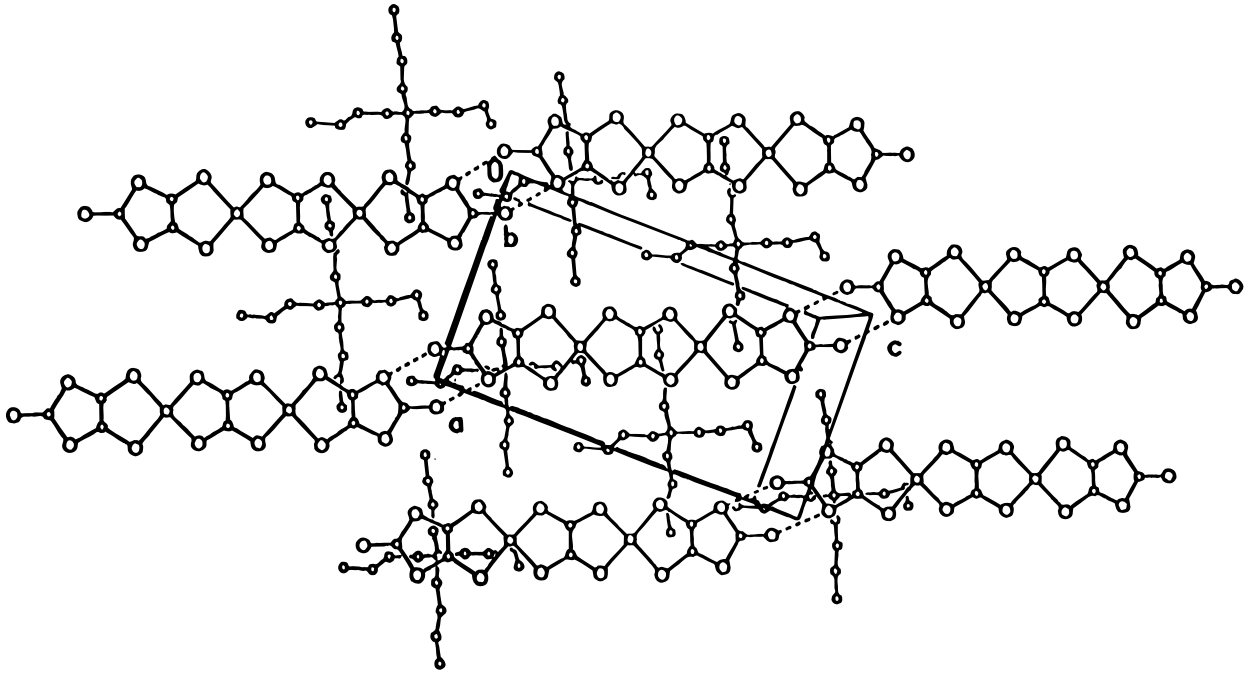

Figure 3. View down the *b* axis of $(Bu_4N)_2\{tto[Ni(dsit)]_2\}$ (**2**) showing one-dimensional chains of the dianionic units formed from head-to-tail thione−thiole nonbonding interactions.

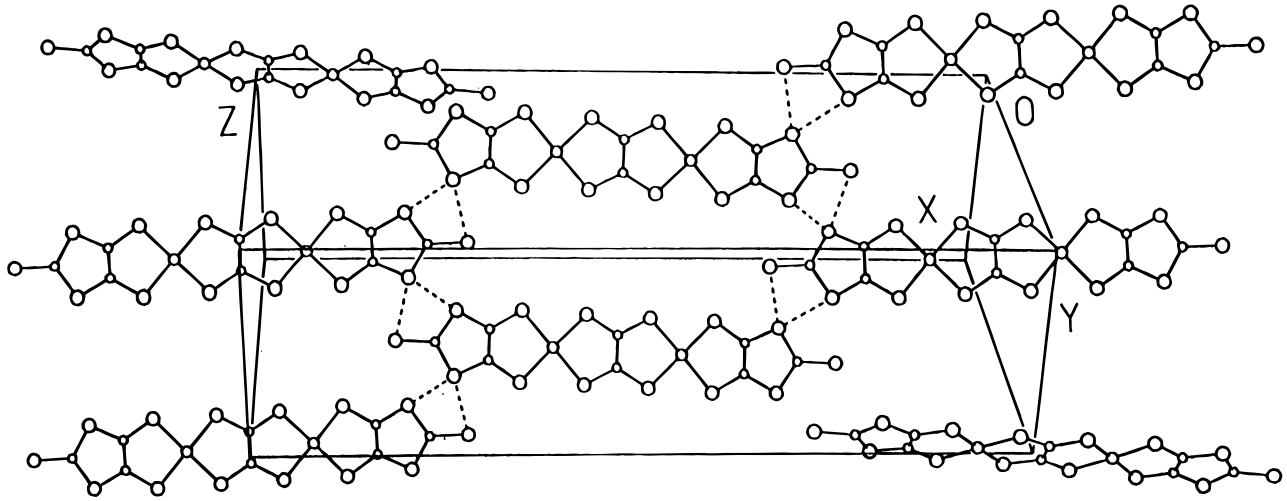

Figure 4. View of $(Bu_4N)_2\{tto[Ni(dmise)]_2\}$ (**3**) showing sheets of dianionic moieties in a two-dimensional array as a result of selenoxo−thiole and thiole−thiole orbital overlap. Tetrabutylammonium cations have been omitted for clarity.

5 with the Et_4N^+ cation, the dihedral angle is very large at 24.5° between the planes of the tto bridging ligand and both capping ligands.

Figure 3 shows a packing diagram of $(Bu_4N)_2\{tto[Ni(dsit)]_2\}$ (**2**), Figure 4 for $(Bu_4N)_2\{tto[Ni(dmise)]_2\}$ (**3**), Figure 5 for $(Me_4N)_2\{tto[Ni(dmit)]_2\}$ (**4**), and Figure 6 for $(Et_4N)_2\{tto[Ni(dmit)]_2\}$ (**5**). In complexes **1**, **2**, and **3**, where the counterions are Bu_4N^+, the packing of the dianions is characterized by one- or two-dimensional sheet-like arrangements separated by sheets of isolated cations. In **3**, the sheets are formed from thiole−thiole (3.448−3.537 Å) and thiole−selenoxo (3.532−3.558 Å) nonbonding interactions in a two-dimensional array. In $(Et_4N)_2\{tto[Ni(dmit)]_2\}$ (**5**), only thiole−thiolato (3.623 Å) orbital interactions are observed in a one-dimensional array. Lastly in $(Me_4N)_2\{tto[Ni(dmit)]_2\}$ (**4**), the small cation tetramethylammonium leads to a three-dimensional packing array of the dianionic units. The units pack in a brick wall like fashion with extensive intermolecular interactions including thiole−thiole (3.577 Å), thiole−thiolato (3.594 Å), and nickel−thioxo (3.454 Å) nonbonding interactions. The intermolecular nonbonding interactions observed are crucial for the formation of completely delocalized metallic-like systems which may lead to materials with highly conducting and possibly superconducting properties. Also, increased interactions are important for the suppression of Peierls lattice distortions inherent in one-dimensional systems.

Redox Properties of $(Bu_4N)_2\{tto[Ni(dmit)]_2\}$ (1), $(Bu_4N)_2\{tto[Ni(dsit)]_2\}$ (2), and $(Bu_4N)_2\{tto[Ni(dmise)]_2\}$ (3). The dianions of complexes **1**−**3** exhibit similar redox behavior. A representative cyclic voltammogram of $(Bu_4N)_2\{tto[Ni(dsit)]_2\}$ (**2**) for all complexes is shown in Figure 7. Cyclic voltammetric data for **1**−**3** is compiled in Table 11.

At beginning potentials of −1.00 V, the compounds are stable in their dianionic form. As seen in the representative cyclic voltammogram during anodic scanning, each complex exhibits a first low-potential redox couple with essentially equal $E_{1/2}$ values at −0.83 V for $(Bu_4N)_2\{tto[Ni(dmit)]_2\}$ (**1**) to −0.82 V for $(Bu_4N)_2\{tto[Ni(dsit)]_2\}$ (**2**) and $(Bu_4N)_2\{tto[Ni(dmise)]_2\}$ (**3**). This first redox couple is reversible as observed peak-to-peak separations are 60−70 mV. Scan rate dependence studies (25−300 mV/s) for this first observed redox process also show that

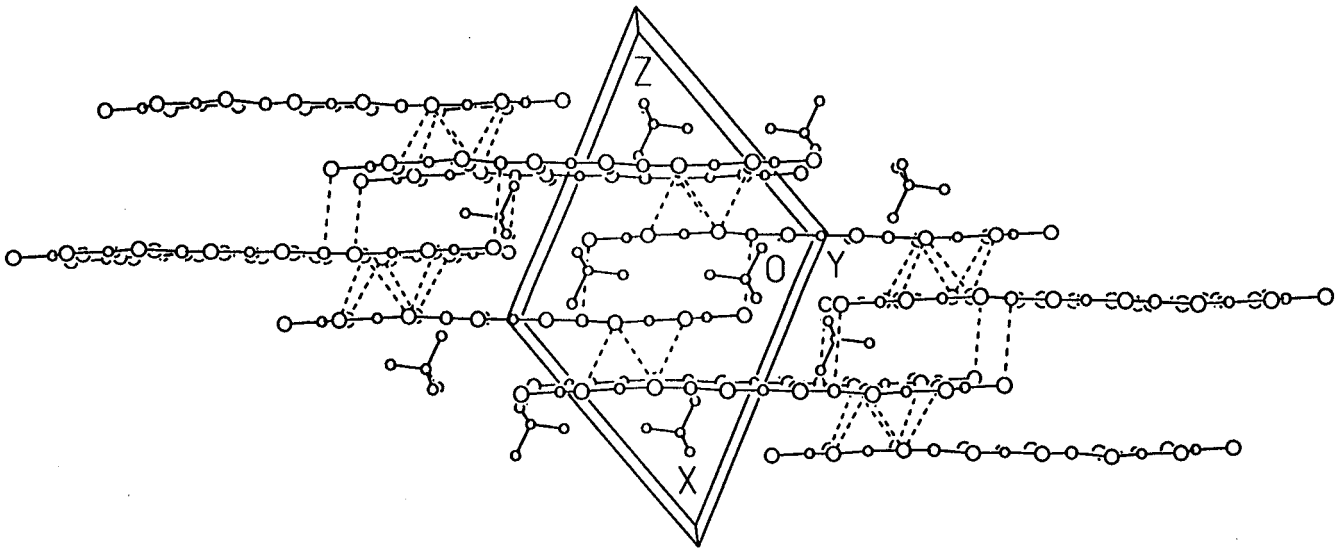

Figure 5. Packing diagram of $(Me_4N)_2\{tto[Ni(dmit)]_2\}$ (**4**) showing multiple nickel-sulfur and sulfur−sulfur nonbonding interactions in a three-dimensional array.

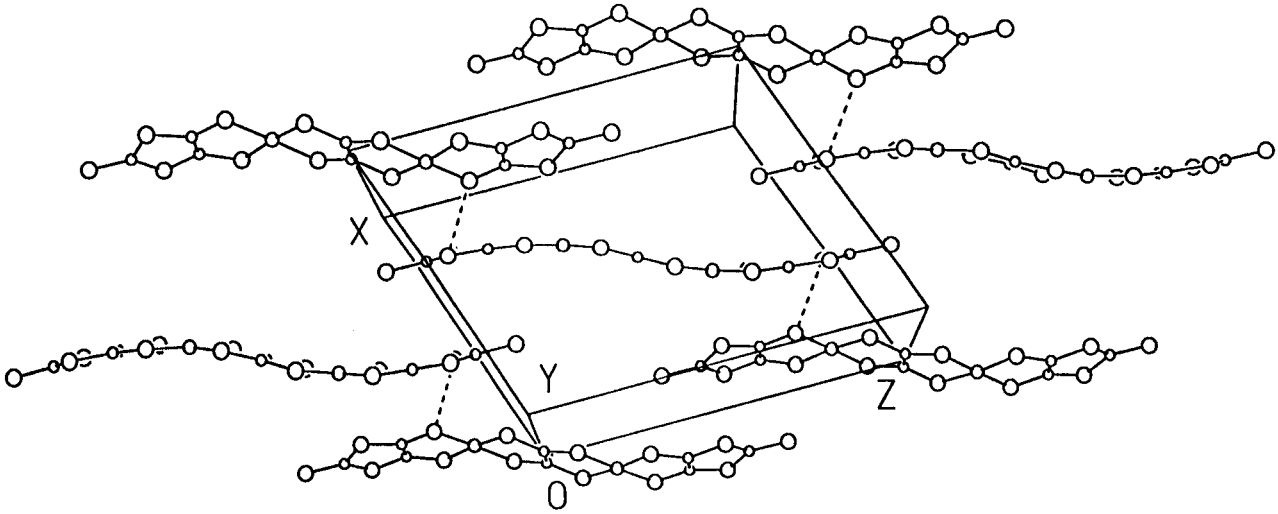

Figure 6. View of $(Et_4N)_2\{tto[Ni(dmit)]_2\}$ (**5**) showing the conformation of the dianionic units. Tetraethylammonium cations have been omitted for clarity.

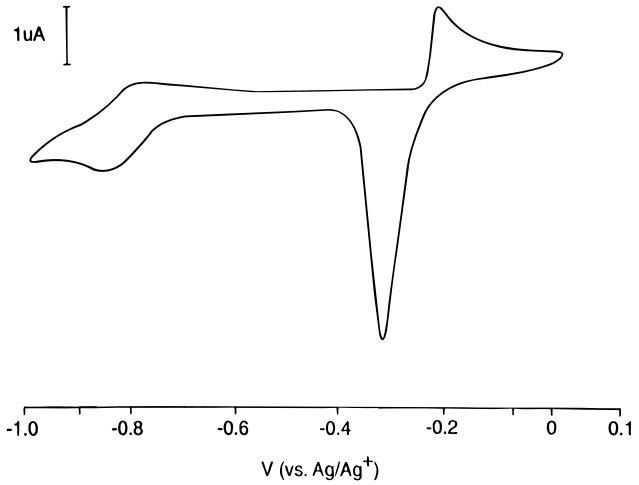

Figure 7. Cyclic voltammogram of $(Bu_4N)_2\{tto[Ni(dsit)]_2\}$ (**2**). Conditions: scan rate, 100 mV/s; reference electrode, Ag/Ag^+; counter electrode, Pt foil; working electrode, Pt button; 0.05 M Me_4NClO_4 in CH_3CN under Ar at room temperature.

the peak currents scale with the square root of the scan rate as anticipated for diffusion of the soluble electroactive species to the electrode surface. This first redox couple seen for all of the complexes can be attributed to a reversible one-electron oxidation process between the dianionic and monoanionic states:

$$\{tto[Ni(L)]_2\}^{2-} \rightleftarrows \{tto[Ni(L)]_2\}^{-}$$

Upon scanning to higher potentials, a second irreversible redox process is observed for all of the complexes. The complex $(Bu_4N)_2\{tto[Ni(dmise)]_2\}$ (**3**) oxidizes at the highest peak potential of −0.15 V to the lowest value observed of −0.23 V for $(Bu_4N)_2\{tto[Ni(dsit)]_2\}$ (**2**). Upon return scanning cathodi-

Table 11. Cyclic Voltammetric Peak Potentials (V) for Complexes $(Bu_4N)_2\{tto[Ni(dmit)]_2\}$ (**1**),[a] $(Bu_4N)_2\{tto[Ni(dsit)]_2\}$ (**2**), and $(Bu_4N)_2\{tto[Ni(dmise)]_2\}$ (**3**)[b]

complex	$E_{p,a}$	$E_{p,c}$	$E_{1/2}$
$(Bu_4N)_2\{tto[Ni(dmit)]_2\}$ (**1**)	−0.80	−0.86	−0.83
	−0.20	−0.25	
$(Bu_4N)_2\{tto[Ni(dsit)]_2\}$ (**2**)	−0.78	−0.85	−0.82
	−0.23	−0.34	
$(Bu_4N)_2\{tto[Ni(dmise)]_2\}$ (**3**)	−0.78	−0.85	−0.82
	−0.15	−0.29	

[a] See ref 8. [b] Conditions: scan rate, 100 mV/s; reference electrode, Ag/Ag^+; counter electrode, Pt foil; working electrode, Pt button; 0.05 M Me_4NClO_4 electrolyte in CH_3CN under Ar at room temperature.

cally, a large reduction peak is observed for all of the complexes with the highest peak reduction potential (−0.25 V) being seen for $(Bu_4N)_2\{tto[Ni(dmit)]_2\}$ (**1**) and the lowest potential of −0.34 V exhibited for $(Bu_4N)_2\{tto[Ni(dsit)]_2\}$ (**2**). The shape of the second redox couple is very similar to the previously reported cyclic voltammetric behavior for the similar $M(dmit)_2$-based bis-chelate and similar derivative complexes $[Ni(dmit)_2]^{2-}$,[17] $[Pd(dmit)_2]^{2-}$,[18] $[Ni(dsit)_2]^{2-}$,[19] and $[Ni(dtdt)_2]^{2-}$ (where dtdt = $C_4H_4S_5^{2-}$ = 5,7-dihydro-1,4,6-trithiin-2,3-dithiolato).[18] The large reduction peak is indicative of a redissolution process. Thorough studies of these types of materials in the mechanism of electrocrystallization have been reported by Cassoux and coworkers[17,18] that show that the large reduction peak observed is due to a redissolution process of deposited noninteger oxidation state material on the electrode surface formed in the diffusion layer. The formation of the deposited material of the bimetallic complexes can best be described by the following:

$$\{tto[Ni(L)]_2\}^- \rightarrow \{tto[Ni(L)]_2\}^{n-} + (1-n)e^-$$

Upon scanning to higher potentials, an increase in current is observed which indicates that the noninteger oxidation state material deposited is electrically conductive. This type of behavior exhibited by the dianions of complexes **1**−**3** plays an important role in the potential formation of highly electrically conducting noninteger oxidation state materials via electrocrystallization and slow-interdiffusion experiments.[17,18]

Electrocrystallization, Slow Interdiffusion, Chemical Oxidation, and Conductivity Experiments. Initial experiments have been carried out using $(Bu_4N)_2\{tto[Ni(dmit)]_2\}$ (**1**) in attempts to synthesize electrically conducting materials via electrocrystallization, slow interdiffusion, and chemical oxidation techniques. Reported in our previous communication, a black precipitate was isolated from the rapid mixing of solutions of a slight excess of $(TTF)_3(BF_4)_2$ and **1** in acetonitrile which had a high pressed-pellet conductivity of 0.4 S/cm.[8] Slow interdiffusion experiments of saturated solutions of $(TTF)_3(BF_4)_2$ and $(Bu_4N)_2\{tto[Ni(dmit)]_2\}$ (**1**) were subsequently carried out. A black precipitate with a conductivity of 0.06 S/cm, as listed in Table 12, was obtained having a stoichiometry of $(TTF)_{0.57}\{tto[Ni(dmit)]_2\}$ as determined by elemental analysis. Using the slow diffusion method, the product has a conductivity approximately an order of magnitude less than that obtained from the rapid mixing of solutions.

Table 12. Pressed Powder Electrical Conductivities of Noninteger Oxidation State Materials Based on tto-Bridged Bimetallic Complexes

complex	σ(S/cm)	synthetic method
$(TTF)_{0.57}\{tto[Ni(dmit)]_2\}$	0.06	rapid mixing
$(TTF)_x\{tto[Ni(dmit)]_2\}$[8]	0.4	slow interdiffusion
$(Bu_4N)_{0.33}\{tto[Ni(dmit)]_2\}$	0.3	rapid mixing
$(Bu_4N)_{0.33}\{tto[Cu(dmit)]_2\}$[7a]	0.01	rapid mixing
$(Bu_4N)_x\{tto[Ni(dmit)]_2\}$	0.5	electrocrystallization

The synthesis of partial oxidation state materials using the $\{tto[Ni(dmit)]_2\}$ anion with Bu_4N^+ as the counterion was also investigated. The rapid mixing of solutions of NaI/I_2 and $(Bu_4N)_2\{tto[Ni(dmit)]_2\}$ (**1**) in acetone yielded a black precipitate of stoichiometry $(Bu_4N)_{0.33}\{tto[Ni(dmit)]_2\}$ as determined by elemental analysis. A conductivity of 0.3 S/cm was found. Similar results were found for $(Bu_4N)_{0.33}\{tto[Cu(dmit)]_2\}$ which was synthesized using the same technique. The conductivity was found to be ∼0.01 S/cm.[7a]

Electrocrystallization experiments of $(Bu_4N)_2\{tto[Ni(dmit)]_2\}$ (**1**) in a mixture of CH_3CN/DMF (4:1) in the presence of Bu_4NBr yielded a black, brittle, microcrystalline material. An approximate stoichiometry could not be determined as the elemental analysis results were ambiguous ($(Bu_4N)_x\{tto[Ni(dmit)]_2\}$). This may be due to solvent molecules being present in the microcrystalline product. Two-probe pressed-powder conductivity measurements were carried out and showed this product to have a conductivity of 0.5 S/cm, the highest observed for noninteger oxidation state materials based on the Ni(II) and Cu(II) bimetallic, tto-bridged complexes.[7,8]

Acknowledgment. This work was funded by grants from the Air Force Office of Scientific Research (F49620-96-1-0067 and F49620-93-1-0322) and a visiting work-study grant from the IAESTE program at the University of Leipzig, Leipzig, Germany (ref #951405-R). K.A.A. wishes to acknowledge the National Science Foundation for funding of the purchase of the X-ray equipment.

Supporting Information Available: Text presenting X-ray experimental details and full tables of crystallographic data, hydrogen atomic coordinates and isotropic thermal parameters, bond lengths and angles, and anisotropic thermal parameters (41 pages). Ordering information is given on any current masthead page.

IC9701219

(17) Tommasino, J. B.; Pomarede, B.; Medus, D.; de Montauzon, D.; Cassoux, P. *Mol. Cryst. Liq. Cryst.* **1993**, *237*, 445.
(18) Faulmann, C.; Errami, A.; Donnadieu, B.; Malfant, I.; Legros, J. P.; Cassoux, P.; Rovira, C.; Canadell, E. *Inorg. Chem.* **1996**, *35*, 3856.
(19) Cornelissen, J. P.; Haasnoot, J. G.; Reedijk, J.; Faulmann, C.; Legros, J. P.; Cassoux, P.; Nigrey, P. J. *Inorg. Chim. Acta* **1992**, *202*, 131.